EXPERIMENTAL AND THEORETICAL STUDIES ON SULFUR DIOXIDE ADSORPTION BY OIL-PALM-SHELL ACTIVATED CARBON

Jia GUO, Aik Chong LUA, and Ting YANG
School of Mechanical and Production Engineering, Nanyang Technological University, Nanyang Avenue, Singapore 639798, Republic of Singapore

Introduction

The global production of sulfur dioxide (SO_2) by human activities (*e.g*. combustion of high-sulfur-content fossil fuels, metal smelting and other industrial processes) is estimated to be 1.4 million tones per year. The amount of emitted SO_2 in the USA, Western Europe and Japan decreases recently, whilst that from the developing countries is increasing gradually [1]. Sulfur dioxide can cause acid rain, which has acidified soils and streams, accelerated corrosion of buildings and reduced visibility. Long-term exposure to SO_2 also results in various respiratory diseases. Many efforts have been taken to eliminate SO_2 emissions or to remove them from flue gases before emitting into the atmosphere. Amongst these techniques, dry removal of SO_2 using adsorbent (particularly activated carbon) is a promising approach that has attracted much attention. This dry method offers distinct advantages of simplicity and economy over wet scrubbing because the later requires high capital investment and operating cost for wastewater treatment facilities [2,3].

Although numerous studies on dry adsorption of SO_2 onto activated carbons have been carried out, this technology has by no means become fully mature. Recently, for economical reasons, interests in using low-cost activated carbons derived from biomass wastes instead of conventional precursors like lignite, peat and coal, have increased. In fact, many solid wastes such as rockrose [4], kraft lignin [5], almond shell [6], cherrystone [7] and olive stone [8] had been successfully converted into effective adsorbents. However, few studies had been reported in the literature pertaining to adsorption of SO_2 onto activated carbons prepared from these biomasses. Arii measured the rate of adsorption and desorption of SO_2 by coconut-based activated carbon with a quartz-spring microbalance, from which an empirical relation to the uptake dynamics was obtained [9]. Strauss investigated the adsorption dynamics of SO_2 on activated carbons from oil fractions, some of which were impregnated with alkali carbonate and alkali sulfate as promoters. Although some of these activated carbons showed good adsorption capacities for SO_2 gas, no adsorption characteristic parameters were extracted from the experimental results [10]. Molina-Sabio *et al*. determined isotherms of SO_2 at 262 and 273K on a series of activated carbons prepared from apricot stones with a wide range of micropore size distributions. The amount of SO_2 adsorbed was found to be a function of the porous texture of the activated carbon [11].

Oil-palm shell (or called *endocarp*) from palm oil processing mills is an agricultural by-products in some tropical countries like Malaysia and Thailand [12]. To make better use of these cheap and abundant wastes, it has been used as starting materials for the preparation of high-quality activated carbons for gas-phase adsorption applications [13,14]. In this study, static and dynamic adsorptions of SO_2 onto the activated carbon prepared from oil-palm shell by physical activation were studied. The effects of adsorption temperature, SO_2 initial concentration, fixed-bed length and gas velocity on the adsorption performance were investigated. Various characteristic parameters were extracted from breakthrough curves obtained during the fixed-bed adsorption process.

Experimental

Oil-palm shells from a palm-oil mill in Selangor, Malaysia were crushed and sieved to the size fraction of 2-2.8 mm. Both carbonization of the raw oil-palm shell and activation of the resulting char were carried out in a stainless-steel reactor, which was placed in a vertical tube furnace (818P, Lenton). During carbonization, the starting materials were heated from normal laboratory temperature (298K) to 873K and held at this temperature for 2 hours under a nitrogen (N_2) flow (150 cm^3/min). The resulting chars were then activated at 1173K for 30 minutes under a carbon dioxide (CO_2) flush of 100 cm^3/min. The characteristics of raw oil-palm shell, char and activated carbon are shown in Table 1.

Static adsorption of SO_2 onto the oil-palm-shell activated carbon was carried out using a thermogravimetric analyzer (TA-50, Shimadzu). SO_2 gas of various concentrations (balanced by N_2) was introduced into the analyzer chamber

where a platinum sample holder containing about 20 mg sample was suspended. The subsequent sample weight gain due to adsorbed SO_2 was recorded. Tests were conducted at different temperatures in order to understand the temperature effect on adsorption.

Dynamic adsorption of SO_2 was conducted in a copper column (10 mm i.d. and 5-30 cm long) filled with activated carbons supporting by a metal mesh at the bottom of the column. Columns were operated in the up-flow mode. SO_2 gas from a cylinder was introduced to the bottom of the adsorption column (inlet) at different volumetric flow rates ranging from 30 to 90 cm^3/min. The respective superficial velocities were 38.2 to 114.6 cm/min. All the runs were carried out at normal laboratory temperature of 298K. The concentration time history at the exit of the column was continually monitored (sampling time < 2s) by a SO_2 gas analyzer (MLT1, Fisher-Rosemount) equipped with a non-dispersive infrared-photometer, followed by a data recording system (LTVTE008, Trendview). The adsorption was performed until saturation, that is, when the outlet concentration equaled the inlet one. A breakthrough curve was then obtained and some characteristic parameters were derived from the curve. The actual weight change due to SO_2 uptake was measured by a microbalance (JK-180, Ohyo).

Results and Discussion

The amounts of SO_2 adsorbed from 2000 ppm SO_2 flow at various temperatures onto the oil-palm-shell activated carbon in the static tests are shown in Figure 1. With increasing adsorption temperature from 298 to 353K, the amounts of SO_2 adsorbed decreased significantly. The reason is that during the adsorption process, the SO_2 molecules lose their kinetic energies, making adsorption an exothermic process [15]. Therefore, the higher the adsorption temperature, the lesser would be the amount adsorbed. If the temperature increases to a certain level (430K for SO_2, which is known as its critical temperature) or even higher, no matter how high the pressure applied to the system is, the gas cannot be liquefied and therefore cannot be adsorbed onto the activated carbon surface [16]. From the thermodynamics point of view, this is due to the extensive thermal vibration of the molecules (or called Brownian movement) at such high temperatures, preventing the adsorbate molecules from being accommodated and attached to the adsorption sites. On the other hand, adsorption at extremely low temperatures (for example adsorption at 77K using liquid nitrogen basin) encounters another problem called “activated diffusion”. Some micropores, which are accessible to adsorbates at room temperature, are not easily occupied by adsorbate molecules since the adsorbates have insufficient kinetic energy to penetrate into the tortuous internal pores [17].

Table 2 shows the effects of inlet SO_2 concentration on the characteristic parameters for static and dynamic adsorption tests. For a low SO_2 concentration of 500 ppm, the amount of SO_2 adsorbed at equilibrium was small (14.8 mg/g) and a long time (115.0 min) was required to reach equilibrium. At a SO_2 concentration of 2000 ppm, the amount adsorbed was as high as 76.3 mg/g and the equilibrium time was only 54.1 min. Such a short equilibrium time suggests a feasible application of these activated carbons for dynamic adsorption in a fixed bed. The characteristic parameters derived from breakthrough curves obtained from dynamic adsorption of 1000 ppm and 2000 ppm SO_2 are also listed in Table 2. In this study, breakthrough time $\tau_{0.05}$ and exhaustion time $\tau_{0.95}$ are defined as the times when the outlet concentrations are at 5% and 95% of the inlet concentration respectively. A shorter breakthrough time and exhaustion time were observed as the inlet SO_2 concentration increased. This means that increasing the inlet concentration, the service time of the fixed bed will be reduced because of a higher loading factor. Table 2 also showed that the actual amount adsorbed in a dynamic adsorption system was much lower than its adsorption in a static system in which equilibrium was attained between the adsorbate and the adsorbent. A similar observation was also reported by Youssef *et al*. when they studied the adsorption of sulfur dioxide onto coal-based activated carbons [18].

In a fixed bed for adsorption, the part that displays a gradient in adsorbate concentration from zero to equilibrium is called the mass transfer zone (MTZ). This is the active part of the bed where adsorption actually takes place. As the saturated part of the bed increases, the MTZ travels downstream and eventually exits the bed. The length of the MTZ (L_{MTZ}) may be estimated using the empirical equations introduced by Pota and Mathews [19]:

$$L_{MTZ} = \frac{L(\tau_{0.95} - \tau_{0.05})}{(\tau_{0.95} + \tau_{0.05})/2} \qquad (1a)$$

where L is the length of the column,
$\tau_{0.05}$ is the breakthrough time, and
$\tau_{0.95}$ is the exhaustion time.

Cheremisinoff and Cheremisinoff [20] proposed an empirical relation which is

$$L_{MTZ} = \frac{L}{\tau_{0.95}(\tau_{0.95} - \tau_{0.05}) - \chi} \qquad (1b)$$

where χ is the degree of saturation in the MTZ (in this study, χ=0 for a clean bed).

Neely and Isacoff [21] derived another expression for L_{MTZ} as follows:

$$L_{MTZ} = \frac{C_0 F}{M\rho_b S}(\tau_{0.95} - \tau_{0.05}) \quad (1c)$$

where C_0 is the inlet adsorbate concentration,
F is the adsorbate gas flow rate,
M is the amount adsorbed at saturation,
ρ_b is the bulk density of the fixed bed, and
S is the cross-sectional area of the adsorption column.

Table 3 shows the length of mass transfer zone estimated from the above equations. For the experimental conditions used in this study, the discrepancies of L_{MTZ} using these equations were really insignificant. The effects of column length on the characteristic parameters derived from the breakthrough curves are shown in Figure 2. For the SO_2 superficial velocity of 63.7 cm/min and inlet concentration of 2000 ppm, increasing column length increased the breakthrough time as well as exhaustion time progressively. However, the column length had an insignificant effect on the L_{MTZ} (2.2±0.1 cm using equation 1a) when the other operating conditions were kept unchanged during all the experimental runs.

For gas-phase adsorption in the fixed bed, the breakthrough time can be expressed using the following semi-empirical equation [22]:

$$\tau_{0.05} = \frac{\rho_b W L}{C_0 u} - \frac{\rho_b W}{C_0 K}\ln\left(\frac{C_0 - C_{0.05}}{C_{0.05}}\right) \quad (2)$$

where W is the adsorption capacity,
u is the gas superficial velocity,
$C_{0.05}$ is the outlet concentration at breakthrough, and
K is the adsorption rate constant.

Equation (2) may be simplified to:

$$\tau_{0.05} = AL + B \quad (3)$$

where $A = \rho_b W / C_0 u$ and $B = -\frac{\rho_b W}{C_0 K}\ln\left(\frac{C_0 - C_{0.05}}{C_{0.05}}\right)$.

Accordingly, $\tau_{0.05}$ plots versus column length (L) should give a straight line. The parameters W and K can be obtained from the values of slope and intercept respectively.

The breakthrough time versus column length for the fixed bed operating at various SO_2 superficial velocities are shown in Figure 3. The slope of the fitted lines decreased with increasing SO_2 superficial velocity. The superficial velocity was proportional to the gas volumetric flow rate, as the column cross-sectional area was constant in all the experimental runs. A smaller gradient implied a lesser amount of SO_2 adsorbed at breakthrough, which was confirmed by the values of adsorption capacity as shown in Table 4. This was as expected because the contact time between SO_2 gas and the adsorbents in the fixed bed decreased with increasing superficial velocity, thereby reducing the amount of gas treated and adsorbed at breakthrough. The relationship between the adsorption capacity (W) and the gas superficial velocity (u) can be expressed empirically as follows (the correlation coefficient r = 0.98):

$$W = 26.0 - 0.16u \quad (4)$$

Another characteristic parameter, adsorption rate constant (K), derived from the breakthrough curve is also listed in Table 4. Increasing the SO_2 superficial velocity from 38.2 to 114.6 cm/min increased the rate constant from 62.4 to 134.0 min^{-1}. This was expected if the rate-limiting step is the external mass transfer of adsorbate molecules to the surface of the activated carbon particle. Generally, the overall mass transfer resistance is approximately expressed by the combination of three mass transfer resistances as follows [23]:

$$\frac{1}{K} = \frac{1}{\beta u} + \frac{1}{K_f} + \frac{1}{K_i} \quad (5)$$

where β is the external mass transfer constant,
K_f is the fluid film mass transfer coefficient, and
K_i is the intraparticle diffusivity.

Figure 4 shows the relationship between the overall mass transfer resistance and the reciprocal of the gas superficial velocity for the dynamic adsorption system. It was clear that the overall mass transfer essentially depended on the gas velocity for the two gas concentrations studied here. Therefore, the external mass transfer resistance was confirmed to be predominant. The result of the best curve fitting for the rate constant (K) and gas superficial velocity (u) is given as (the correlation coefficient r = 0.91):

$$K = 5.6u^{0.68} \quad (6)$$

The same dependence of superficial velocity on rate constant was also found in other fixed-bed adsorption tests [19,22,23]. However, theoretically, the rate constant should be proportional to the square root of the gas velocity [24].

Conclusions

The following conclusions could be drawn from the experimental and theoretical studies on sulfur dioxide adsorption onto the oil-palm-shell activated carbons.

1) With increasing adsorption temperature in the range of 298 to 353K, the amounts of SO_2 adsorbed onto the activated carbon decreased significantly due to the

exothermic nature of the adsorption process. Temperature higher than the critical temperature of the adsorbate resulted in no adsorption whilst too low a temperature might result in an "activated diffusion" phenomenon.

2) For the static adsorption test, with increasing SO_2 concentration, the amount adsorbed increased and the equilibrium time was shortened. For dynamic adsorption in a fixed bed, a shorter breakthrough time and exhaustion time were observed as the inlet SO_2 concentration increased. The actual amount adsorbed from a dynamic adsorption system was much lower than its adsorption from a static system in which equilibrium was attained between the adsorbate and the adsorbent.

3) The length of mass transfer zone is an important parameter for the fixed bed adsorption system. There were no significant differences found amongst the three empirical equations used for estimating L_{MTZ}. Under the same experimental conditions, the effect of column length on L_{MTZ} was also insignificant.

4) The adsorption capacity was found to be inversely proportional to the gas superficial velocity. The relationship between the rate constant and the gas superficial velocity was also obtained. This confirmed that the external mass transfer was the rate limiting step of the whole adsorption process.

References

1. Mochida I, Korai Y, Shirahama M, Kawano S, Hada T, Seo Y, Yoshhikawa M, Yasutake A. Carbon 2000;38:227-39.
2. Rubio B, Izquierdo MT. Carbon 1997;35(7):1005-11.
3. Lu GQ. Environ Progress 1996;15(1):12-8.
4. Pastor-Villegas J, Valenzuela-Calahorro C, Bernalte-Garcia A, Gomez-Serrano V. Carbon 1993;31(7):1061-9.
5. Rodriguez-Mirasol J, Cordero T, Rodriguez JJ. Carbon 1993;31(1):87-95.
6. Marcilla A, Garcia-Garcia S, Asensio M, Conesa JA. Carbon 2000;38:429-40.
7. Lussier MG, Shull JC, Miller DJ. Carbon 1994;32(8):1493-8.
8. Gonzalez MT, Rodriguez-Reinoso F, Garcia AN, Marcilla A. Carbon 1997;35(1):159-65.
9. Arii K. Bull Inst Phys Chem Res 1935;14:1210-32.
10. Strauss W. In: Proc 2nd Int Clean Air Congr, New York: Academic Press, 1970, p.130.
11. Molina-Sabio M, Munecas MA, Rodriguez-Reinoso F, McEnaney B. Carbon 1995;33(12):1777-82.
12. Yeoh GB, Idrus AZ, Ong KS. ASEAN J Sci Technol Develop 1988;5(1):1-13.
13. Guo J, Lua AC. J Oil Palm Res 2000;12(1):64-70.
14. Lua AC, Guo J. Colloids Surface A 2001;179:151-62.
15. Yang RT. Gas Separation by Adsorption Processes, Boston: Butterworths, 1987, p.26.
16. Gray PG. Gas Sep Purifi 1993;7(4):213-24.
17. Pandolfo AG, Aminz-Amoli M, Killingley JS. Carbon 1994;32(7):1015-9.
18. Youssef AM, Mostafa MR, Dorgham EM. Adsorption Sci Tech 1997;15(10):803-14.
19. Pota AA, Mathews AP. J Environ Eng 1999;705-12.
20. Cheremisinoff NP, Cheremisinoff PN. Carbon Adsorption for Pollution Control, New Jersey: PTR Prentice Hall, 1993, p.90.
21. Neely JW, Isacoff EG. Carbonaceous Adsorbents for the Treatment of Ground and Surface Waters, New York: Marcel Dekker, 1982, p.107.
22. Wood GO, Stampfer JF. Carbon 1993;31(1):195-200.
23. Takeuchi Y, Hino M, Yoshimura Y, Otowa T, Izuhara H, Nojima T. Sep Purifi Technol 1999;15:79-90.
24. Busmundrud O. Carbon 1993;31(2):279-86.

Table 1. Physical characteristics of raw oil-palm shell, char and activated carbon

Sample	Solid density [a] (g/cm^3)	Apparent density [b] (g/cm^3)	Porosity [c] (%)	BET surface area [d] (m^2/g^1)	Micropore surface area [e] (m^2/g^1)
Oil-palm shell	1.53	1.47	3.9	1.6	0.2
Char	1.63	1.35	17.2	176	108
Activated carbon	2.03	0.69	66.0	1366	958

a. Measured by an ultra-pycnometer (UPY-1000, Quantachrome).
b. Measured by a mercury intrusion porosimeter (PoreSizer-9320, Micromeritics).
c. Calculated from (solid density – apparent density) / solid density × 100%.
d. Measured by an accelerated surface area and porosimeter (ASAP-2000, Micromeritics).
e. Calculated based on the micropore volume obtained by using Dubinin-Radushkevich (DR) equation.

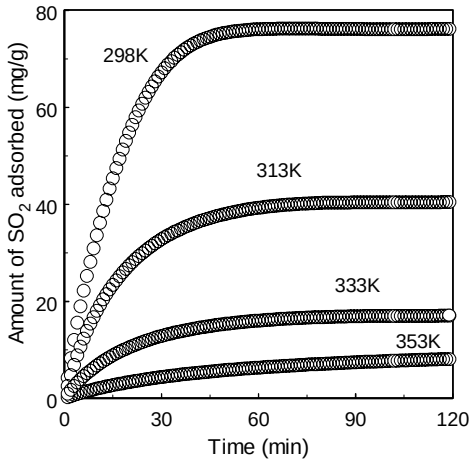

Figure 1. Effects of adsorption temperature on the amount of SO_2 adsorbed for static adsorption.

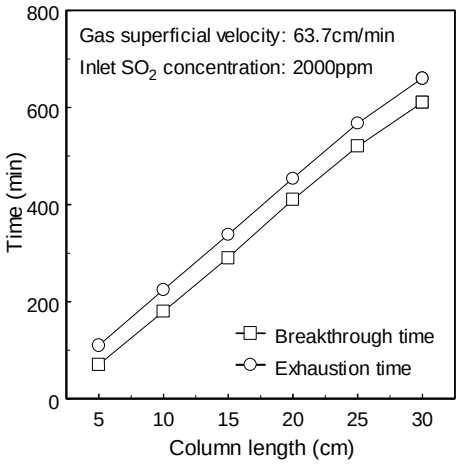

Figure 2. Effects of column length on the characteristic parameters for dynamic adsorption.

Table 2. Effects of inlet concentration on the characteristic parameters for static and dynamic adsorption tests

Inlet SO_2 concentration (ppm)	Amount adsorbed for static adsorption (mg/g)	Equilibrium time for static adsorption (min)	Actual amount adsorbed for dynamic test (mg/g)	Breakthrough time for dynamic adsorption (min)	Exhaustion time for dynamic adsorption (min)
500	14.8	115.0	—	—	—
1000	35.2	87.4	11.7	203.8	245.6
2000	76.3	54.1	24.9	181.4	224.7

Table 3. Estimation of the length of mass transfer zone (L_{MTZ}) based on different empirical equations

Inlet SO_2 concentration (ppm)	Column length (cm)	SO_2 superficial velocity (cm/min)	Adsorption temperature (K)	Reference No.	Length of mass transfer zone (cm)
2000	10	63.7	298	[19]	2.1
				[20]	1.9
				[21]	2.0

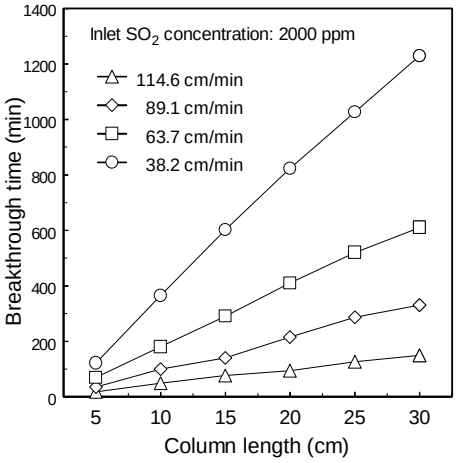

Figure 3. A plot of breakthrough time versus bed length for the fixed bed operating at various SO_2 superficial velocities.

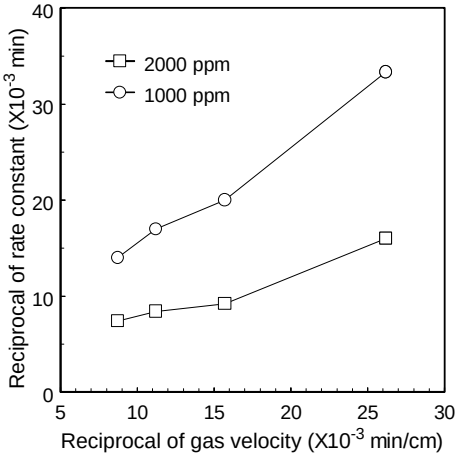

Figure 4. A plot of the reciprocal of rate constant versus the reciprocal of gas velocity for different inlet concentrations.

Table 4. Effects of gas superficial velocity on the characteristic parameters for dynamic adsorption

SO_2 superficial velocity (cm/min)	Adsorption capacity, W (mg/g)	Rate constant, K (min^{-1})
38.2	19.3	62.4
63.7	16.0	110.2
89.1	12.3	118.9
114.6	6.8	134.0